Scintigraphic Tracking of ^{99m}Technetium Labelled Equine Peripheral Blood-Derived Mesenchymal Stem Cells After Intravenous, Intramuscular and Subcutaneous Injection in Healthy Dogs.

Charlotte Beerts
Global Stem cell Technology
Carlien Brondeel
University of Ghent: Universiteit Gent
Glenn Pauwelyn
Global Stem cell Technology
Eva Depuydt
Global Stem cell Technology
Liesa Tack
Global Stem cell Technology
Luc Duchateau
University of Ghent: Universiteit Gent
Yangfeng Xu
University of Ghent: Universiteit Gent
Jimmy H. Saunders
University of Ghent: Universiteit Gent
Kathelijne Peremans
University of Ghent: Universiteit Gent
Jan H. Spaas (jan.spaas@anacura.com)
Global Stem cell Technology https://orcid.org/0000-0002-6683-2593

Research

Keywords: Mesenchymal stem cells, xenogeneic, equine peripheral blood, scintigraphy, biodistribution, canine

Posted Date: October 28th, 2020

DOI: https://doi.org/10.21203/rs.3.rs-95566/v1

Version of Record: A version of this preprint was published at Stem Cell Research & Therapy on July 13th, 2021. See the published version at https://doi.org/10.1186/s13287-021-02457-9.

Abstract

Background: Mesenchymal stem cell treatments in dogs have been investigated as a potential innovative alternative to current conventional therapies for a variety of conditions. So far, the precise mode of action of the MSCs has yet to be determined. The aim of this study was to gain more insights in the pharmacokinetics of MSCs by evaluating their biodistribution in healthy dogs after different injection routes.

Methods: Three different studies were performed in healthy dogs to evaluate the biodistribution of radiolabelled equine peripheral blood-derived mesenchymal stem cells following intravenous, intramuscular and subcutaneous administration in comparison with free ^{99m}Technetium. The labelling of the equine peripheral blood-derived mesenchymal stem cells was performed using stannous chloride as reducing agent. Whole body scans were obtained using a gamma camera during a 24h follow-up.

Results: The labelling efficiency ranged between 59.58 and 83.82%. Free ^{99m}Technetium accumulation was predominantly observed in stomach, thyroid, bladder and salivary glands while, following intravenous injection, the ^{99m}Technetium labelled equine peripheral blood-derived mesenchymal stem cells majorly accumulated in the liver throughout the follow-up period. After intramuscular and subcutaneous injection, the injected dose percentage remained very high at the injection site.

Conclusions: A distinct difference was noted in biodistribution of the radiolabelled equine peripheral blood-derived mesenchymal stem cells compared to free ^{99m}Technetium indicating equine peripheral blood-derived mesenchymal stem cells have a specific pharmacokinetic pattern after systemic administration in healthy dogs. Furthermore, the natural biodistribution pattern of the used equine peripheral blood-derived mesenchymal stem cells appeared to be different to previously reported experiments using different sources of mesenchymal stem cells.

Background

Over the past decade the use of mesenchymal stem cell (MSC) treatments in dogs has been investigated as an interesting and innovative alternative to current conventional therapies. Promising results were described for a variety of conditions such as osteoarthritis, tendon and ligament lesions, liver diseases, atopic dermatitis and inflammatory bowel disease [1, 2, 3, 4, 5, 6, 7, 8]. The most frequently used sources of canine MSCs are autologous or allogeneic adipose tissue derived MSCs. Other available sources include autologous synovial fluid-derived MSCs, autologous or allogeneic bone marrow-derived MSCs, allogeneic umbilical cord-derived MSCs and xenogeneic equine peripheral blood-derived MSCs [1, 3, 4]. Allogeneic and xenogeneic MSCs are a more attractive source than the autologous MSCs which have to be harvested from the tissue of each patient and put into culture before being available. Xenogeneic MSCs are an interesting alternative for use in dogs since canine MSCs have culture and upscaling limitations caused by senescence earlier in the culture process than for example in human and equine MSCs [9, 10, 11].

MSCs are capable of differentiating in different cell lineages, have immunomodulatory effects, and stimulate local repair cells by paracrine signals [12, 13, 14]. However, additional studies are requested to further define their mode of action. The evaluation of the biodistribution of MSCs would help to gain more insights in their pharmacokinetics. Spriet, Spriet, Hunt et al. described the scintigraphic tracking of ^{99m}Technetium-hexamethyl-propylene amine oxime (HMPAO) labelled allogeneic adipose tissue-derived MSCs following portal, intravenous and splenic administration in four healthy dogs. To the authors' knowledge, the study conducted by Spriet, Hunt et al., is the only one describing the distribution of ^{99m}Tc labelled MSCs in dogs [15]. Scintigraphic tracking of MSCs was also reported in horses and human [16, 17, 18, 19, 20].

In most of these studies MSCs were labelled using HMPAO as chelating agent to bind ^{99m}Technetium to the MSCs [16, 18, 19, 20] and one group used a combination of HMPAO and stannous chloride for the MSCs labelling [17]. Our group recently reported the labelling of equine peripheral blood-derived mesenchymal stem cells (ePB-MSCs) for scintigraphic tracking after intravenous administration in horses using stannous chloride ($SnCl_2$) for the labelling of the MSCs (paper submitted). In the study reported by Spriet, Buerchler et al. in 2015, an intravenous regional limb perfusion and a subcutaneous injection in the metacarpal area or the coronary band were performed in horses. The subcutaneous injection resulted in a loss of the MSCs to the general circulation however there was no evidence of local migration [19]. To the author's knowledge, no study has described the biodistribution of subcutaneously injected MSCs in dogs.

The aim of this study was to evaluate the biodistribution of ^{99m}Technetium labelled equine MSCs, in comparison with free ^{99m}Technetium, after intravenous (IV), intramuscular (IM) and subcutaneous (SC) application in healthy dogs.

Methods

Experiments

Three different studies were performed. In a first study, the biodistribution of intravenously administrated ePB-MSCs was evaluated in four dogs. In the second study, the biodistribution of intramuscularly and subcutaneously administrated ePB-MSCs was evaluated in four dogs. Finally, in a third study, the biodistribution of a higher dose of ePB-MSCs following intravenous administration was evaluated in three dogs.

Animals

The different animal studies (approval number EC: 2019_003 and 2019_006) and the blood collection of the donor horses (approval number: EC_2016_003) were approved by the ethics committee of Global Stem cell Technology. The ethics committee is approved by the Flemish government with permit LA1700607. The study was good clinical practice compliant (VICH GL9) and all animal handlings were conducted according to European, national and regional animal welfare regulations (Directive 2001/82/EC as amended, Belgian animal welfare legislation (KB 29/05/2013), Directive 2010/63/EU and EMEA/CVMP/816/00-Final).

Four healthy adult research dogs were included in the two first studies; three dogs from the second study were re-used for the third study. All dogs were purpose bred adult beagles (16-23 months). Two males and two females were included in the first two studies and one male and two female dogs were included in the third study. The dogs were housed in groups of 2, in a pen of 4 by 4 by 2 m (L x W x H) so permanent visual, olfactorial, tactile and auditive contact between dogs was possible. Toys were provided for the dogs to play with in their pen. Cleaning of the dog pens was performed daily. The floor was covered with wood shavings to improve lying comfort for the dogs. The animals were let out in dog runs to play and run for minimal 1 hour a day. After the study this minimal time was increased depending on the need of the dogs.

A daily general physical assessment was performed for each study evaluating the following parameters: rectal temperature, respiratory rate, heart rate, mucosal membranes, capillary refill time, body conditions score, mentation and hydration.

Control product preparation

For the preparation of the control product (CP), 20 ± 5 millicurie (mCi) (740 ± 185 megabecquerel (MBq)) of freshly eluted 99mTc Pertechnetate (99m Tc) from a molybdenum generator (GE health care, Eindhoven, The Netherlands) was added to 1 mL of Dulbecco's Modified Eagle low glucose Medium (DMEM) (Life Technologies Europe BV, Belgium).

Collection and culture of ePB-MSCs

As previously described by our group [21], the ePB-MSCs were good manufacturing practices (GMP) manufactured in a GMP-certified site (number: BE/GMP/2018/123). Briefly, blood was taken from the jugular vein of a donor horse (approval number EC: EC_2012_001 and 2016_003) and the MSCs were isolated. The serum was analyzed for a range of transmittable diseases by Böse laboratory (Harsum, Germany). As already described by our group [11], the blood was centrifuged and the buffy coat was collected for gradient centrifugation. After washing, the ePB-MSCs were cultivated until passage 5 and a characterization for viability, morphology, presence of cell surface markers and population doubling time was performed. Next the ePB-MSCs were frozen as an intermediate cell stock. When characterization was completed, the intermediate cell stock was thawed and cultivated until passage 10 before being trypsinezed, resuspended, filtered twice trough a 40 µm filter and vialed at $3x10^5$ cells/mL in a mixture of DMEM and 10% dimethylsulfoxide (DMSO). The vials were stored at -80°C until further use.

^{99m} Tc-labelling of the ePB-MSCs

The technique of ^{99m}Tc labelling the ePB-MSCs was based on an optimization study recently described by our group (paper submitted). First, stannous chloride powder (Sigma Aldrich, US) was dissolved in sterile basic water (pH 8.5). Next, 0.9 x 10^6 ePB-MSCs were thawed in the hand palm, transferred into growth medium and centrifuged for pelleting. The cell pellet was then re-suspended in 4 mL of saline and mixed with 5 µg $SnCl_2$ and 45 ± 5 mCi (1665 ± 185 MBq) of freshly eluted ^{99m}Tc from a molybdenum generator (GE health care, Eindhoven, The Netherlands). Next the preparation was incubated for 30 minutes at room temperature before being centrifuged. The cell pellet was washed with 5 mL DMEM and centrifuged again. The final cell pellet was resuspended in 1 mL of DMEM and the viability of the ePB-MSCs following the labelling was determined using trypan blue. The radioactivity of the supernatant was measured after each centrifugation step in a dosiscalibrator and used to calculate the labelling efficiency.

Treatment

In the first study, each dog received two intravenous injections; first the dogs were injected with the control product: freshly eluted ^{99m}Tc dissolved in DMEM and at least 7 days later they received a second injection with ^{99m}Tc-labelled ePB-MSCs. For the second study, 4 injections were administered to each dog. The dogs first received an IM injection with the control product, next a SC with the control product, then an IM injection with the ^{99m}Tc-labelled ePB-MSCs and finally a SC administration of the ^{99m}Tc -labelled ePB-MSCs. At least 7 days separated each injection. In the third study, the three dogs received a single IV injection with ^{99m}Tc-labelled ePB-MSCs.

The dogs were put under general anesthesia and positioned in sternal recumbency on the gamma camera before each injection. To obtain general anesthesia, the dogs were first sedated with dexmedetomidine (12-25 µg/kg IM), next induction was obtained with propofol (dosage on effect) and anesthesia was maintained with isoflurane 1.2-1.4% (on effect) in 100% oxygen following endotracheal intubation. The intravenous injection was administered through a 22-gauge catheter in one of the cephalic veins, the intramuscular injection was performed in the left quadriceps muscle and the subcutaneous injection was administered at the back of the neck.

Imaging protocol

A two-headed gamma camera, equipped with low energy high resolution collimators (GCA 7200 A; Toshiba) was used for the scintigraphic investigation. The whole body scan was obtained with the detectors of the SPECT scanner moving simultaneous dorsally and ventrally from head to tail of the dog over 10 minutes. All dogs were kept under general anesthesia during all the acquisitions. For all 3 studies, data collection of the first hour consisted of 6 successive acquisitions of each 10 minutes. The start of the first acquisition was simultaneous with injection of the radioactive compound and the dog remained in the same position for all 6 scans. Next, in the first study, total body scans (each lasting 10 minutes) were performed at 2h, 4h, 8h, 12h, 24h and 36h after placebo control and labelled ePB-MSCs administration using propofol (dosage on effect). For the second and the third study, 6 successive 10 minutes' total body scans performed during the first hour after injection were followed by total body scans (each lasting 10 minutes) at 6h and 24h after each injection. For all studies, a syringe with a known amount of radioactivity to calculate % injected dose (ID), was simultaneous scanned with the dog. Care was taken for the dog's re-positioning on the table, to avoid too much spatial deviation on the scans following the first hour scans.

Image interpretation

First, the distribution of the placebo control and the labelled ePB-MSCs was assessed descriptively through the whole body. Consequently, the radioactivity was quantified in different manually drawn regions of interest (ROI) on the dorsal and ventral view of the whole body scans (matrix size 512x1024) using the free-hand region of interest tool of a DICOM viewing software platform (Hermes MultiModalityTM, Nuclear Diagnostics, Sweden). A geometric mean of dorsal and ventral activity for each time point and each ROI was calculated to compensate for attenuation. Relative uptake was expressed as % of decay corrected injected activity for each region of interest per time point and calculated based on the known standard activity. To keep shape and sizes (number of pixels) of the different organ ROI's uniform, a ROI template was created per study and per dog and used for the different time points. A specific organ ROI was drawn on the image on which the organ was best delineated and thereafter used for the other images. Due to minor positioning deviations in between scans, ROI's had to be replaced on some images, however without changing the shape and size.

Due to the low sample size of four animals, only the overall effects in the heart, lung, liver and bladder following intravenous injection were taken into account for statistical analysis. The data were analyzed with SAS® statistical analysis software (version 9.4, SAS Institute Inc., Cary, NC, USA). For the intramuscular and subcutaneous injections no statistical analysis was performed since a high radioactivity uptake remained at the injection sites following the injections of the radiolabelled ePB-MSCs and only a descriptive evaluation seemed appropriate. The overall statistical difference between intravenous administration of the free 99mTc and the radiolabelled ePB-MSCs in the heart, lungs, liver and bladder was calculated using the area under the curve (AUC). The AUC was calculated using the trapezoidal method and can be written as a weighted sum of the observations. To allow a better interpretation of the AUC, it was presented as the weighted mean of the observations, using the weights of the observations in the AUC sum. A paired t-test was performed for this AUC for each organ separately, using the dog as a block effect. The time effects were described descriptively. The normality distribution assumption of the residuals was tested using the Shapiro-Wilks test and could not be rejected.

Results

Control product preparation

The injected ^{99m}Tc activity for the CP injection in each dog is displayed in Table 1.

Table 1

^{99m}Tc **activity and route of the CP injected to each dog in the different studies**

Study	Dog	Injection Route	Injected ^{99m}Tc activity (mCi)
1	1	IV	20.04
	2		22.55
	3		22.70
	4		19.26
2	6	IM	18.60
	7		25.00
	8		22.45
	9		21.24
	6	SC	18.15
	7		21.50
	8		20.60
	9		18.96
mCi: millicurie, IV: intravenous, IM: intramuscular, SC: subcutaneous			

Labelling efficiency, post-labelling viability and injected dose

For the first study, the mean (min-max) overall labelling efficiency was 64.76% (59.58 – 71.50 %), the number of MSCs ranged between 305,000 and 415,000 and post-labelling cell viability amounted to 84.64% (79.10 – 88.52 %). For the IM injection of the second study, a mean overall labelling efficiency of 69.37% (53.65 – 77.83 %), 465,000 to 775,000 MSCs and post-labelling cell viability of 93.70% (90.32 – 96.96 %) were obtained and for the SC administration of the same study, the mean overall labelling efficiency was 72.94% (66.21 % - 78.34 %), the number of MSCs per sample was 730,000 to 825,000 and post-labelling cell viability was 94.96 % (93.63 – 96.96 %). Finally, a mean overall labelling efficiency of 82.50% (80.65 – 83.82 %), 1,610,000 to 1,950,000 MSCs and a cell viability of 95.40% (93.17 – 97.44 %) were obtained in the third study (Table 2).

Table 2
Injection route, 99mTc activity, labelling efficiency, number and viability of the labelled-ePB-MSCs injected to each dog in the different studies

Study	Dog	Injection Route	Injected ^{99m}Tc activity (mCi)	Labelling efficiency (%)	Number of MSCs	Viability of MSCs (%)
1	1	IV	17.36	71.50	415,000	87.95
	2		17.64	59.58	305,000	88.52
	3		19.40	67.80	385,000	83.00
	4		16.38	60.15	335,000	79.10
2	5	IM	18.45	72.78	465,000	90.32
	6		19.05	73.21	775,000	95.48
	7		24.04	77.83	695,000	93.53
	8		15.00	53.65	775,000	95.48
	5	SC	15.62	66.21	825,000	96.96
	6		20.15	69.18	785,000	93.63
	7		23.38	78.02	760,000	94.74
	8		23.49	78.34	730,000	94.52
3	6	IV	19.56	80.65	1,810,000	95.58
	7		27.85	83.04	1,950,000	97.44
	8		21.37	83.82	1,610,000	93.17

mCi: millicurie, IV: intravenous, IM: intramuscular, SC: subcutaneous

Safety

The parameters rectal temperature, respiratory rate, heart rate, mucosal membranes, capillary refill time, body conditions score, mentation and hydration were in the physiological range for all animals at all time points of observation. No abnormal general clinical signs were observed and no (serious) adverse events or suspected adverse drug reactions were observed during the study.

Biodistribution

Intravenous injection of the CP led to an accumulation of free ^{99m}Tc in the following organs: heart, lung, liver, stomach, bladder, thyroid and salivary glands. Following intramuscular and subcutaneous administration of the placebo control, radioactivity uptake was seen in the heart, lung, stomach, bladder, thyroid and salivary glands. The highest uptake was seen in the stomach for all three injection routes with a progressive increase until 4 to 6 hours post-injection. (Table 3, Figure 1). In the first study, the scintigraphic examination 36 hours post-injection was performed, however the radioactive counts were too low to quantify. Therefore, this time point was not included for the evaluation of the biodistribution.

Table 3
Average percentage of injected dose observed in the different organs 10 minutes, 60 minutes, 6 hours and 24 hours following intravenous, intramuscular and subcutaneous injection of the control product.

	10 min			60 min			6 hours			24 hours		
	IV	IM	SC	IV	IM	SC	IV	IM	SC	IV	IM	SC
Heart	2.79	0.45	0.24	1.61	2.46	1.61	1.45	1.45	1.61	0.54	0.69	0.70
Lung	3.73	1.06	0.92	2.62	6.92	4.86	1.97	4.41	4.57	0.77	2.14	2.01
Liver	2.93	/	/	2.07	/	/	1.73	/	/	0.99	/	/
Stomach	4.84	1.62	0.53	9.77	17.36	9.24	8.98	17.25	14.37	5.02	9.36	7.32
Bladder	0.63	0.13	0.13	1.93	3.51	2.29	2.42	4.77	2.75	2.71	5.08	3.75
Thyroid	0.41	0.05	0.00	0.61	1.10	0.00	0.61	1.15	0.96	0.24	0.57	0.61
Left Salivary Gland	0.33	0.02	0.12	0.77	1.03	0.45	1.31	1.84	1.44	1.34	2.47	2.67
Right Salivary Gland	0.33	0.01	0.13	0.72	0.99	0.45	0.88	1.60	1.33	0.98	2.09	2.81
Injection Site	/	29.49	27.27	/	3.63	17.57	/	0.19	0.00	/	0.12	0.00

IV: intravenous, IM: intramuscular, SC: subcutaneous

Following intravenous injections of the normal and the higher dose of the labelled ePB-MSCs into the cephalic vein of the dogs, presence was predominantly observed in the heart, lung, liver and bladder. Furthermore, minor radioactive uptake was seen in the spleen and kidneys. The highest uptake was seen in the liver with stable radioactivity until 24 hours post-injection. Intramuscular injection of the labelled ePB-MSCs led to a low radioactivity uptake in the following organs: lung, liver and kidneys. High uptake remained at the injection site for the entire evaluation period. This uptake at the injection site masked a potential uptake in the bladder. Finally, after subcutaneous injection of the labelled ePB-MSCs, low radioactivity uptake in the following organs was seen: kidneys and bladder. Again, high uptake remained at the injection site for the entire evaluation period. Radioactive uptake could be seen in the liver, however, this uptake was too low to be quantified. The uptake at the injection site masked a potential uptake in the heart and/or lung (Table 4, Fig. 2).

Table 4
Average percentage of injected dose observed in the different organs 10 minutes, 60 minutes, 6 hours and 24 to 36 hours following intravenous, intramuscul subcutaneous injection of the radiolabelled ePB-MSCs

	10 min				60 min				6 hours				24 hours			
	IV	IV+	IM	SC	IV	IV+	IM	SC	IV	IV+	IM	SC	IV	IV+	IM	SC
Heart	1.88	2.00	/	/	1.19	1.38	/	/	0.70	0.94	/	/	0.33	0.71	/	/
Lung	5.77	10.64	0.00	/	3.63	6.33	0.03	/	1.90	3.91	0.00	/	1.30	3.20	0.00	/
Liver	22.52	22.38	/	/	23.27	23.21	/	/	22.07	27.26	/	/	19.71	25.30	/	/
Spleen	0.91	1.58	/	/	0.87	1.95	/	/	0.85	2.23	/	/	0.76	2.21	/	/
Left Kidney	0.74		0.00	0.00	0.66		0.06	0.03	0.75		0.08	0.06	0.35		0.09	0.22
Bladder	0.94	0.12	/	0.00	3.49	1.08	/	0.28	5.54	1.28	/	23.57	0.59	1.67	/	28.02
Injection Site	/	/	33.76	23.74	/	/	31.08	23.73	/	/	40.42	14.67	/	/	44.95	35.07

IV: intravenous (normal dose: IV, higher dose: IV+), IM: intramuscular, SC: subcutaneous

A significant difference (P-value = 0.003) for ID% in the liver between the free ^{99m}Tc and radiolabelled ePB-MSCs could be found following IV administration. No significant difference was obtained following both IV injections in the heart (p = 0.28), lung (p = 0.58) or bladder (p = 0.21) (Fig. 3).

Discussion

The different studies describe the total body distribution of intravenously, intramuscularly and subcutaneously injected ^{99m}Tc labelled ePB-MSCs compared with free ^{99m}Tc during a 24 h follow-up period with scintigraphy in healthy dogs. To the authors' knowledge this is the first study comparing the biodistribution of ^{99m}Tc labelled ePB-MSCs with free ^{99m}Tc in dogs. Furthermore, a total body scintigraphy after intravenous, intramuscular and subcutaneous injection of ^{99m}Tc labelled ePB-MSCs has never been described.

The labelling efficiency and cell viability ranged between 59.58% and 83.82% and between 79.10% and 97.44% for all studies, respectively. This is considerably higher than the labelling efficiency of 42 to 57% reported by Spriet, Hunt et al. where the MSCs were labelled with 99mTc-HMPAO. However, no post-labelling cell viability was reported for this study [15].

Free ^{99m}Tc is preferentially taken up by the stomach, thyroid gland and salivary glands [22]. This was also seen in the current studies for the different injection routes (i.e. IM, SC and IV). No radioactive accumulation was observed in none of these organs at all time points following the different injections routes of ^{99m}Tc -labelled ePB-MSCs. Therefore, we could confirm the used ^{99m}Tc labelling technique resulted in a stable *in vivo*-complex with ePB-MSCs. Additionally, the labelling did not affect viability of the ePB-MSCs after injection, since it is assumed that cell death would cause a release of ^{99m}Tc since the cell membrane is no longer intact and accumulate in the aforementioned organs similar to free ^{99m}Tc injections. A lower uptake of free ^{99m}Tc was seen in the heart and lung following all injections and in the liver after intravenous injection. Finally, the previously described partial excretion route of ^{99m}Tc through glomerular filtration explains the increased uptake in the bladder [22].

No pronounced initial pulmonary trapping of the ePB-MSCs following the different injection routes was seen. In the third study, more ID % was detected in the lungs, however, this can be explained by the higher amount of cells injected. There was initial accumulation in the lungs after injecting the higher dose, indicating no long-term entrapment of the ePB-MSCs occurs after IV injection. In contrast, other groups using technetium-labelled mesenchymal stem cells described initial high pulmonary trapping [15, 23]. The absence of pulmonary entrapment in the current studies could be explained by the use of a different MSC source and a lower number of injected MSCs. In the study reported by Spriet et al., 10×10^6 adipose tissue-derived MSCs were injected in the same dog breed as in our studies, whereas our group injected only 305,000 to 1,950,000 equine peripheral blood-derived MSCs in the dogs. Moreover, a part of the production process of the ePB-MSCs used in this study consists of a filtration process reducing the risk of cell clustering following the intravenous injection of the ePB-MSCs.

In contrast to the observations reported by Spriet, Hunt et al., a high liver uptake was seen following both intravenous injections (i.e. study 1 and study 3) of the ePB-MSCs which remained stable during the first 6 hours following the injection and only decreased slightly 24 hours post injection [15]. These findings support the potential use of intravenously administered ePB-MSCs for the treatment of liver diseases such as acute liver injuries or hepatocutaneous syndrome [6, 8].

Following IM and SC injection only a very low biodistribution of the radiolabelled ePB-MSCs was seen and a high amount of the injected MSCs stayed at the injection site throughout the 24-hour follow-up period. Consequently, the biodistribution of the ePB-MSCs following IM and SC injections appears to be different from intravenously injected ePB-MSCs.

The limitations of the studies were the absence of blinding and randomization. Blinding was not feasible because the wash out period of the radiolabelled ePB-MSCs is currently unknown and therefore could not be administered first before the free ^{99m}Tc This practical constraint together with the reported knowledge on distribution of free ^{99m}Tc in literature [22], would have meant that the investigator could have guessed with high certainty which animals would have received the free ^{99m}Tc and which ones the radiolabelled ePB-MSCs when evaluating the total body scans. However, the absence of blinding was mitigated by using an objective evaluation criterion for evaluation of biodistribution i.e. scintigraphic total body scans for quantifying radioactivity in a region of interest instead of using subjective scores. Another limitation was the low number of dogs included in the studies which limited the possibilities for statistical analysis.

Conclusions

This study describes the biodistribution of radiolabelled ePB-MSCs following intravenous, intramuscular and subcutaneous injection in dogs measured by scintigraphic evaluation of radioactivity. During this study a distinct difference was noted in biodistribution of the radiolabelled ePB-MSCs and free ^{99m}Tc. This implies ePB-MSCs have a specific pharmacokinetic pattern after systemic administration in healthy animals. This study thus gives indications for more targeted sampling during safety studies. Additionally, it also provided information on the natural biodistribution pattern of the used ePB-MSCs which appeared to be different to previously reported experiments using different MSC sources.

Abbreviations

MSC: Mesenchymal stem cell

HMPAO: Hexamethyl-propylene amine oxime

ePB-MSCs: Equine peripheral blood-derived mesenchymal stem cells

SnCl2: Stannous chloride

IV: Intravenous

IM: Intramuscular

SC: Subcutaneous

99m Tc: 99mTc Pertechnetate

mCi: Millicurie

DMEM: Dulbecco's Modified Eagle low glucose Medium

MBq: Megabecquerel

GMP: Good manufacturing practices

DMSO: Dimethylsulfoxide

ID: Injected dose

ROI: Regions of interest

AUC: Area under the curve

Declarations

Ethics approval and consent to participate

The different animal studies (approval number EC: 2019_003 and 2019_006) and the blood collection of the donor horses (approval number: EC_2016_003) were approved by the ethics committee of Global Stem cell Technology. The ethics committee is approved by the Flemish government with permit LA1700607. The study was good clinical practice compliant (VICH GL9) and all animal handlings were conducted according to European, national and regional animal welfare regulations (Directive 2001/82/EC as amended, Belgian animal welfare legislation (KB 29/05/2013), Directive 2010/63/EU and EMEA/CVMP/816/00-Final).

Consent for publication

Not applicable.

Availability of data and materials

The datasets used and/or analysed during the current study are available from the corresponding author on reasonable request.

Competing interests

CB, ED, GP, LT and JHS[1,2] are all employed by GST. JHS is an inventor of a pending patent covering the described immunomodulating technology owned by GST (EP19162270.3). EDP, CB and JHS[1,2] are the inventors of a patent covering the ^{99m}Tc labelling of ePB-MSCs owned by GST (EP19200152.7). The content of this manuscript contains a stem cell product under development owned by GST. The other authors declare no competing interests.

Funding

The authors declare that this study received funding from Global Stem cell Technology (GST) NV. The funder had the following involvement with the study: study design, data collection and analysis, decision to publish and preparation of the manuscript.

Authors' contributions

CB[1,2], CB[2] and JHS[1,2] conceived and planned the design of the study. ^{99m}Tc labelling was performed by CB[1,2], ED, LT and GP. IV, IM and SC ePB-MSCs administration, animal handling and scintigraphy was performed by CB[1,2], CB[2], YX and KP. KP analyzed and quantified the scintigraphy images. CB[1,2], CB[2], GP and KP interpreted the data, managed the literature research and wrote the first draft of the manuscript. LD performed the statistical analysis. JHS[1,2] and JHS[2] provided supervision and critical review of the manuscript. All authors contributed and approved the final version of the manuscript.

Acknowledgements

Not applicable.

References

1. Daems R, Van Hecke L, Schwarzkopf I, Depuydt E, Broeckx SY, David M, Beerts C, Vandekerckhove P, Spaas JH. Feasibility Study on the Use of Equine Chondrogenic Induced Mesenchymal Stem Cells as a Treatment for Natural Occurring Osteoarthritis in Dogs. Stem Cells Int. 2019; 2019:4587594. doi: 10.1155/2019/4587594.

2. Gardin C, Ferroni L, Bellin G, Rubini G, Barosio S, Zavan B. Therapeutic Potential of Autologous Adipose-Derived Stem Cells for the Treatment of Liver Disease. Int J Mol Sci. 2018; 19(12):4064. doi: 10.3390/ijms19124064.

3. Gugjoo MB, Amarpal A, Sharma GT. Mesenchymal stem cell basic research and applications in dog medicine. J Cell Physiol. 2019;234(10):16779-16811. doi:10.1002/jcp.28348

4. Hoffman AM, Dow SW. Concise Review: Stem Cell Trials Using Companion Animal Disease Models. Stem Cells. 2016; 34: 1709-1729. doi:10.1002/stem.2377.

5. Muir P, Hans EC, Racette M, Volstad N, Sample SJ, Heaton C, Holzman G, Schaefer SL, Bloom DD, Bleedorn JA, Hao Z, Amene E, Suresh M, Hematti P. Autologous Bone Marrow-Derived Mesenchymal Stem Cells Modulate Molecular Markers of Inflammation in Dogs with Cruciate Ligament Rupture. PLoS One. 2016;11(8):e0159095. doi: 10.1371/journal.pone.0159095.

6. Nam A, Han SM, Go DM, Kim DY, Seo KW, Youn HY. Long-Term Management with Adipose Tissue-Derived Mesenchymal Stem Cells and Conventional Treatment in a Dog with Hepatocutaneous Syndrome. J Vet Intern Med. 2017;31(5):1514-1519. doi: 10.1111/jvim.14798.

7. Pérez-Merino EM, Usón-Casaús JM, Zaragoza-Bayle C, Duque-Carrasco J, Mariñas-Pardo L, Hermida-Prieto M, Barrera-Chacón R, Gualtieri M. Safety and efficacy of allogeneic adipose tissue-derived mesenchymal stem cells for treatment of dogs with inflammatory bowel disease: Clinical and laboratory outcomes. Vet J. 2015;206(3):385-90. doi: 10.1016/j.tvjl.2015.08.003.

8. Yan Y, Fang J, Wen X, Teng X, Li B, Zhou Z, Peng S, Arisha AH, Liu W, Hua J. Therapeutic applications of adipose-derived mesenchymal stem cells on acute liver injury in canines. Res Vet Sci. 2019; 126:233-239. doi: 10.1016/j.rvsc.2019.09.004.

9. Bertolo A, Steffen F, Malonzo-Marty C, Stoyanov J. Canine mesenchymal stem cell potential and the importance of dog breed: implication for cell-based therapies. Cell Transplantation. 2015; 24: 1969–1980. doi:10.3727/096368914X685294.

10. Bertolo A, Schlaefli P, Malonzo-Marty C, Baur M, Pötzel T, Steffen F, Stoyanov J. Comparative Characterization of Canine and Human Mesenchymal Stem Cells Derived from Bone Marrow. Int J Stem cell Res Ther. 2015;2(1):1–6. doi: 10.23937/2469-570X/1410005.

11. Spaas JH, Schauwer C De, Cornillie P, Meyer E, Soom A, Van de Walle GR. Culture and characterisation of equine peripheral blood mesenchymal stromal cells. Vet J. 2013;195(1):107–13. doi:10.1016/j.tvjl.2012.05.006.

12. Baraniak PR, McDevitt TC. Stem cell paracrine actions and tissue regeneration. Regen Med. 2010; 5, 121-143. doi:10.2217/rme.09.74

13. Nöth U, Steinert AF, Tuan, R.S. Technology insight: adult mesenchymal stem cells for osteoarthritis therapy. Nat Clin Pract Rheumatol 2008; 4, 371-380. doi:10.1038/ncprheum0816.

14. Yun S, Ku SK, Kwon YS. Adipose-derived mesenchymal stem cells and platelet-rich plasma synergistically ameliorate the surgical-induced osteoarthritis in Beagle dogs. J Orthop Surg Res 2016.; 11, 9. doi:10.1186/s13018-016-0342-9.

15. Spriet M, Hunt GB, Walker NJ, Borjesson DL. Scintigraphic tracking of mesenchymal stem cells after portal, systemic intravenous and splenic administration in healthy beagle dogs. Vet Radiol Ultrasound. 2015;56(3):327-34. doi: 10.1111/vru.12243.

16. Barberini DJ, Aleman M, Aristizabal F, Spriet M, Clark KC, Walker NJ, Galuppo LD, Amorim RM, Woolard KD, Borjesson DL. Safety and tracking of intrathecal allogeneic mesenchymal stem cell transplantation in healthy and diseased horses. Stem Cell Res Ther 2018;9(1):1–11. doi: 10.1186/s13287-018-0849-6.

17. Becerra P, Valdés Vázquez MA, Dudhia J, Fiske-Jackson AR, Neves F, Hartman NG, Smith RK. Distribution of injected technetium(99m)-labeled mesenchymal stem cells in horses with naturally occurring tendinopathy. J Orthop Res. 2013;31(7):1096–102. doi: 10.1002/jor.22338.

18. Patel CD, Agarwal S, Seth S, Mohanty S, Aggarwal H, Gupta N. Detection of homing-in of stem cells labeled with technetium-99m hexamethylpropyleneamine oxime in infarcted myocardium after intracoronary injection. Indian J Nucl Med 2014;29(4):276–7. doi: 10.4103/0972-3919.142647.

19. Spriet M, Buerchler S, Trela JM, Hembrooke TA, Padgett KA, Rick MC, Vidal MA, Galuppo LD. Scintigraphic tracking of mesenchymal stem cells after intravenous regional limb perfusion and subcutaneous administration in the standing horse. Vet Surg. 2015;44(3):273-80. doi: 10.1111/j.1532-950X.2014.12289.x.

20. Trela JM, Spriet M, Padgett KA, Galuppo LD, Vaughan B, Vidal MA. Scintigraphic comparison of intra-arterial injection and distal intravenous regional limb perfusion for administration of mesenchymal stem cells to the equine foot. Equine Vet J. 2014;46(4):479–83. doi:10.1111/evj.12137.

21. Broeckx S. Tenogenesis of Equine Peripheral Blood-Derived Mesenchymal Stem Cells: In vitro Versus In vivo. J Tissue Sci Eng. 2012;S11:1–6. doi: 10.4172/2157-7552.S11-001.

22. Mettler FA, Guiberteau MJ. Radioactivity, Radionuclides, and Radiopharmaceuticals. Essentials Nucl Med Mol Imaging. 2019 doi:10.1016/B978-0-323-48319-3.00001-8.

23. Meseguer-Olmo L, Montellano AJ, Martínez T, Martínez CM, Revilla-Nuin B, Roldán M, Mora CF, López-Lucas MD, Fuente T. Intraarticular and intravenous administration of ^{99M}Tc-HMPAO-labeled human mesenchymal stem cells (9^{9M}TC-AH-MSCS): In vivo imaging and biodistribution. Nucl Med Biol. 2017;46:36–42. doi: 10.1016/j.nucmedbio.2016.12.003.

Figures

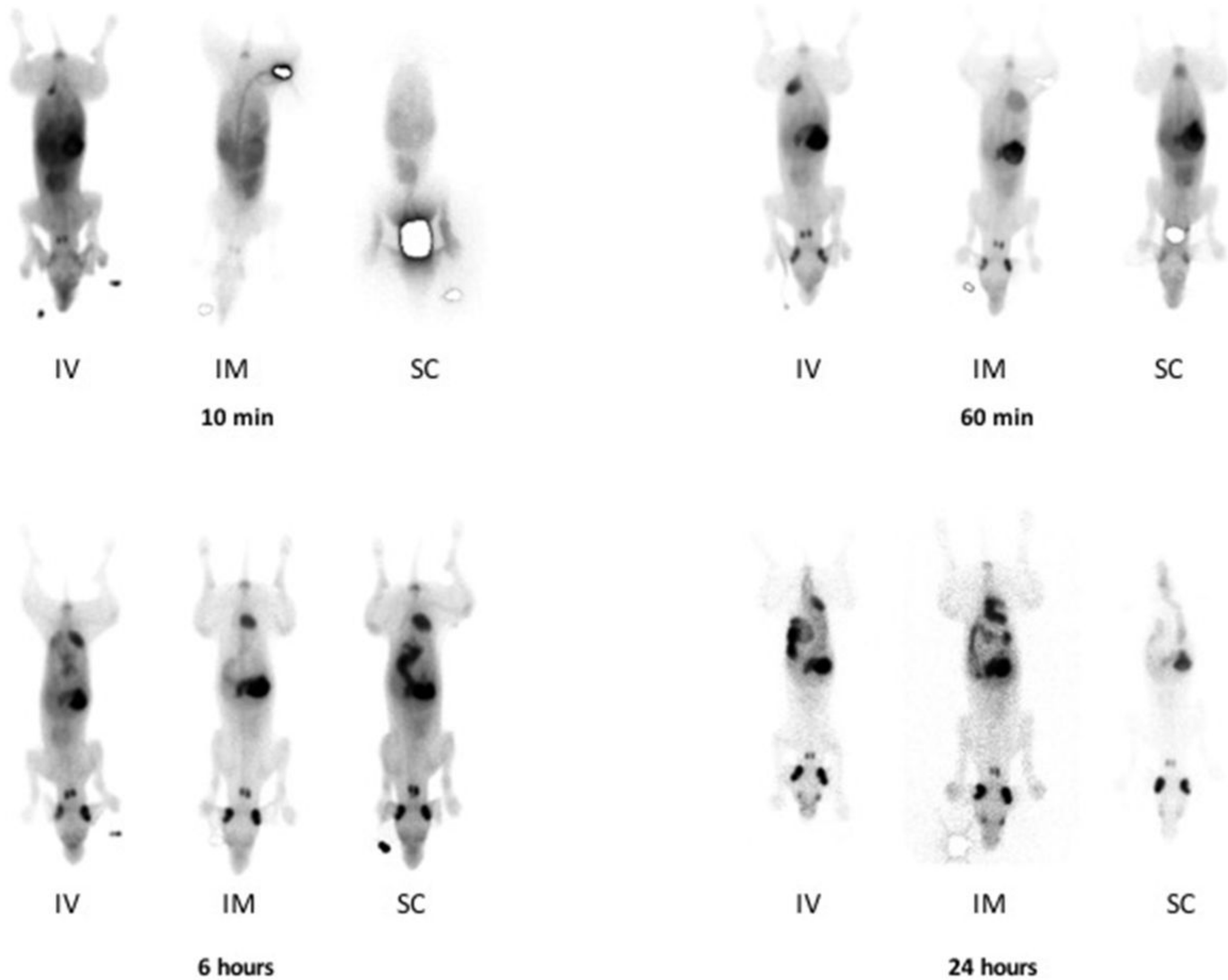

Figure 1

Measured radioactivity 10 minutes, 60 minutes, 6 hours and 24 hours following intravenous, intramuscular and subcutaneous injection of the control product. Following IV, IM and SC administration of the in 99mTc dissolved in DMEM, the heart, lung, stomach (and intestines on the later time points), thyroid, salivary glands and urinary bladder can be seen. Activity in injection site is masked on the 10 minute views of IM and SC and on the 60 minutes view of the SC administration.

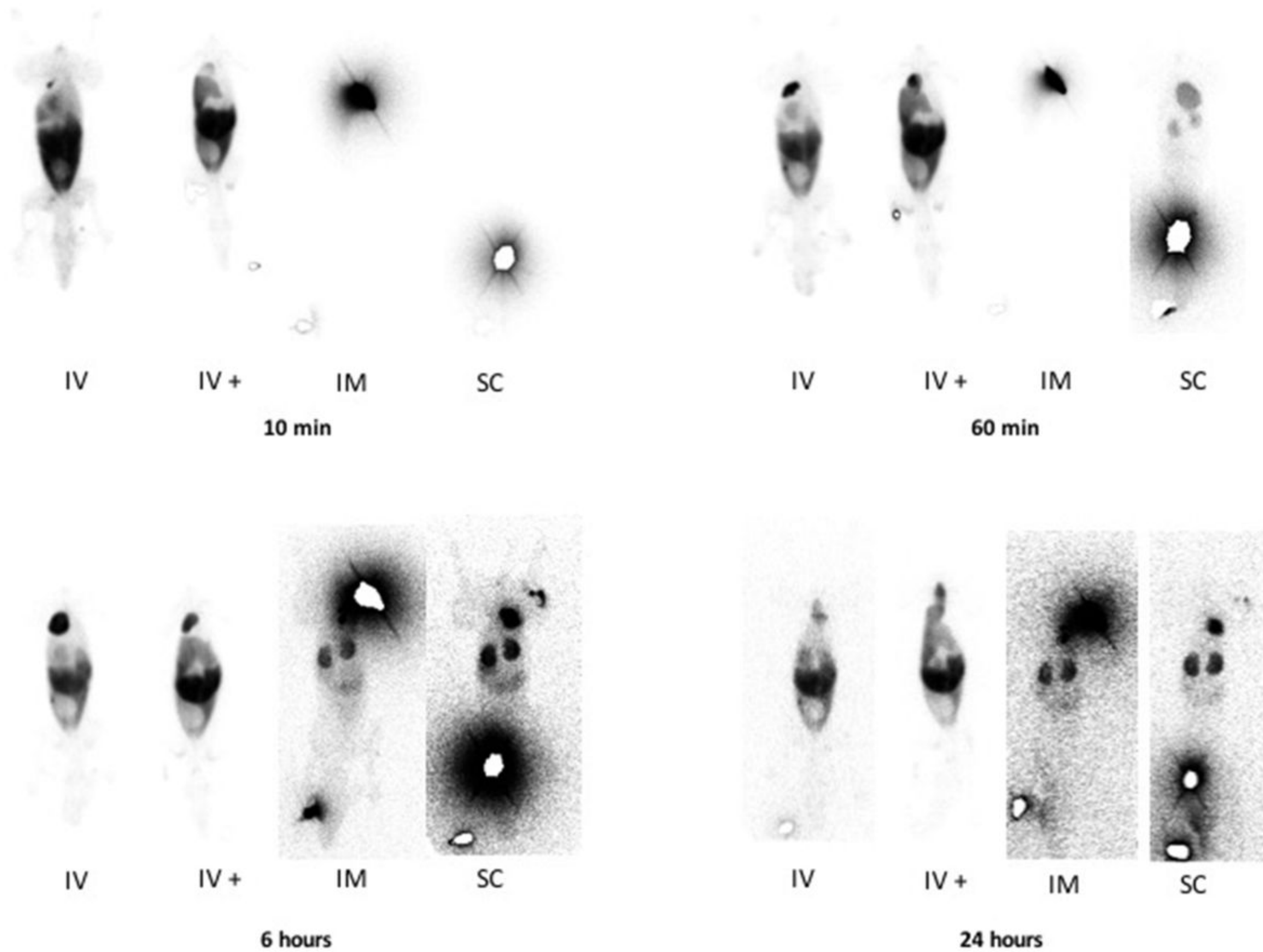

Figure 2

Measured radioactivity 10 minutes, 60 minutes, 6 hours and 24 hours following intravenous (normal dose: IV, higher dose: IV+), intramuscular (IM) and subcutaneous (SC) injection of the radiolabelled ePB-MSCs. Following intravenous administration of ePB-MSCs labeled with 99mTc, the heart, lung, liver, spleen, kidneys, and urinary bladder can be seen. Following intramuscular injection of the ePB-MSCs radiolabeled with 99mTc, the liver and, kidneys can be seen. The injection site in the quadriceps muscle is clearly visible until the end of the evaluation period. Following subcutaneous injection of the ePB-MSCs radiolabeled with 99mTc, the liver, kidneys and bladder can be seen. The injection site in the neck is clearly visible until the end of the evaluation period.

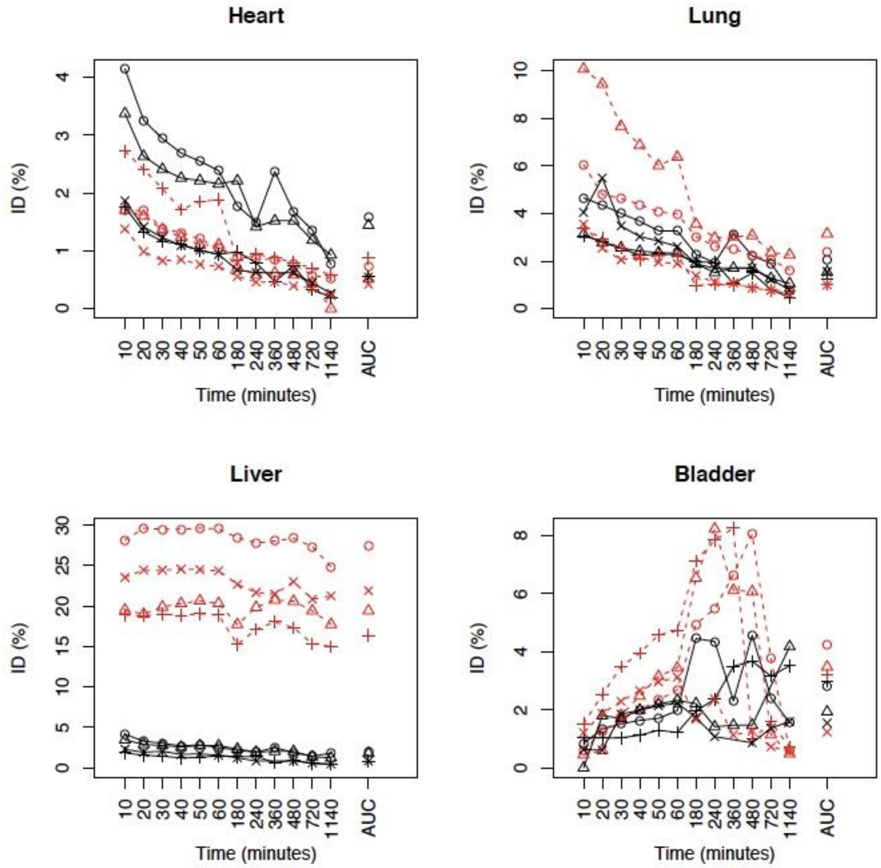

Figure 3

Evolution over time in the heart, lung, liver and bladder for each dog following intravenous injection of free 99mTc (black) and radiolabelled ePB-MSCs (red). A significant difference (P-value= 0.003) for ID % in the liver between the free 99mTc and radiolabelled ePB-MSCs could be found following IV administration. No significant difference was obtained following both IV injections in the heart (p = 0.28), lung (p = 0.58) or bladder (p = 0.21).